7

AC ELECTRICAL PROPERTIES OF INSULATOR-CONDUCTOR COMPOSITES

T. A. Ezquerra, F. Kremer, and G. Wegner

7.1 Introduction

The necessity of light materials having the attractive mechanical properties of common polymers and the electrical conductivities of metals is a scientific and industrial challenge. Insulator-Conductor composites have been subject of experimental and theoretical studies for a long time [1,2]. In particular carbon black and carbon fiber composites are two of the most actively investigated systems due to the

broad application in the automobile and aerospace industry [3,4,5]. As far as electrical properties are concerned, the attention has been mainly focused on the direct current (dc) properties due to the increasing use of carbon black composites for dissipating static charge. Percolation theory has been used to describe the insulator to conductor transition present in this type of materials [6,7,8]. More recently the employ of conducting composites for electromagnetic shielding and as capacitive video disk units [9] has turned the interest on the alternating current (ac) electrical properties of composites. The basic understanding of the processes governing the charge transport under alternating fields in percolation clusters is a matter of permanent interest [10]. Ac experiments performed on composite systems are needed in order to test the different mechanism of charge transport as for instance anomalous diffusion in percolation clusters [11].

7.2 Experimental Techniques

When an electrical field is applied to a dielectric medium a displacement of the electric charge occurs which is characterized by the electric displacement vector $\vec{D}$. There is a phase shift between $\vec{D}$ and $\vec{E}$ giving rise to a complex constant of proportionality [12] between both vectors in the form:

$$\vec{D} = \epsilon^* \epsilon_0 \vec{E} \tag{1}$$

where $\epsilon^* = \epsilon' - i\epsilon''$ is the complex relative permittivity or dielectric constant of the material and ϵ_0 the permittivity of the free space. The variation with time of the vector $\vec{D}$ is related to the current density by one of the Maxwell's laws as:

$$rot\vec{H} - \frac{d\vec{D}}{dt} = \vec{J} \tag{2}$$

where

$$\vec{J} = \sigma^* \vec{E} \tag{3}$$

is the current density, $\sigma^* = \sigma' - i\sigma''$ is the complex electrical conductivity and $\vec{H}$ the magnetic field. The real and imaginary terms of ϵ^* have a physical meaning which can be understood when the dielectric is considered to fill a capacitor [13].

Thus if an external oscillating field $\vec{E} = \vec{E}_0 e^{i\omega t}$ is applied to the sample, the current density:

$$\vec{J} = \epsilon^* \epsilon_0 \frac{d\vec{E}}{dt} = i\omega\epsilon^* \epsilon_0 \vec{E} = \epsilon_0 \vec{E}\omega(\epsilon'' + i\epsilon') = \vec{J}_R + i\vec{J}_C \qquad (4)$$

where ϵ_0 is the vacuum dielectric constant, $\vec{J}_c = \omega\epsilon_0\epsilon'\vec{E}$ the capacitive component of the current and $\vec{J}_R = \omega\epsilon_0\epsilon''\vec{E}$ is the resistive component. Comparing with (3) the following relations for conductivity are obtained:

$$\sigma' = \omega\epsilon_0\epsilon'' \qquad (5)$$

$$\sigma'' = -\omega\epsilon_0\epsilon' \qquad (6)$$

σ' is normally referred as ac (alternating current) conductivity and ϵ' as the relative permittivity. Both components of the complex permittivity ϵ' and ϵ'' can be experimentally measured and characterize the dielectric dispersion of a given material in a particular range of frequencies. As far as composite materials are concerned, frequencies up to 300 GHz (λ = 1mm) are of potential interest. In addition a strong characteristic absorption appearing at visible frequencies in suspensions of of metallic particles has been reported [14].

a. Measurements in the Range $10 - 10^7$ *Hz Impedance Analyzers*

Between 0.01 kHz and 10 MHz Impedance analyzers are commonly used to study relaxation processes in polymers [15,16] and liquid crystals [17]. In particular they can be used to evaluate electric conductivity and dielectric constant of composite materials.

A 4192A HP Impedance Analyzer typical experimental set up is shown in Fig. 7.1. An electric alternating potential field is applied over the sample. At zero adjustment, where the bridge current $I_d = 0$ it follows that:

$$I_x = I_r \qquad (7)$$

and hence the complex impedance of the sample Z is:

$$Z_x = R_r e_s e_r^{-1} \qquad (8)$$

where e_s and e_r are complex voltages (Fig. 7.1). The material can be regarded as an equivalent circuit consisting of a capacitance C and

a resistance R in parallel [13]. The total impedance of the circuit is given by:

$$\frac{1}{Z} = \frac{1}{R} + i\omega C \tag{9}$$

The out-of-phase capacitive component of the current I_c = imaginary part $(\frac{V}{Z}) = \omega$ CV and the in-phase resistive current term I_R = real part $(\frac{V}{Z}) = \frac{V}{R}$ can be evaluated. Consequently by comparing with (6) the following expressions for the components of the complex dielectric constant can be obtained as:

$$\epsilon' = \frac{C}{C_0}, \epsilon'' = \frac{1}{RC_0\omega} \tag{10}$$

The resistive component of the current is directly linked with the resistance and, thus, with the conductivity σ' of the specimen defined as the reciprocal of the resistance of a unit cube of the material. For a given geometry (A = surface area of the sample, s = thickness of the sample) $C_0 = \epsilon_0 \frac{A}{s}$ and $\sigma' = \frac{s}{A}\frac{1}{R}$. The commonly referred as dielectric constant is the real part ϵ' of the complex dielectric function. A similar analysis can be done by considering an equivalent circuit consisting of a capacitance and a resistance in series [13]. The sample preparation for the measurements depends on the conductivity of the material. For low conducting materials a two electrodes sandwich geometry is commonly used. The sample is placed in a parallel plate capacitor [13,18,19,20]. Metallic electrodes are evaporated or painted on both sample faces. Guard ring electrodes are employed in order to avoid surface current effects. For conductivities higher than 10^{-5} S/cm (1 S/cm = $ohm^{-1}cm^{-1}$) the contact resistance at the sample surface is not negligible as compared with the volumen resistance. In this case a four electrode configuration allows to obtain accurate conductivity measurements [21]. There exist several arrangements depending on the nature of the system under study [22,23,24]. The most standard disposition consists on four collinear electrodes [13] in which a current density is supplied to the sample through the outer electrodes. The potential drop is measured across the two inner electrodes. The experimental accuracy in this frequency range is for a dielectric material with dc conductivity $\sigma_{dc} < 10^{-11}$S/cm about $\pm 1\%$ in ϵ'. For materials of medium dc conductivity of about 10^{-5} S/cm the accuracy on ϵ'' and ϵ' and hence in σ' and σ'' is comparable. For materials of higher conductivity with the four electrode configuration a lower accuracy of

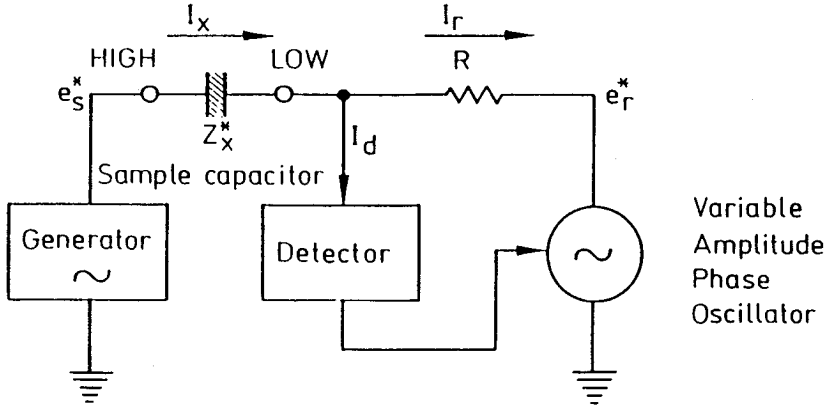

Figure 7.1 Experimental set-up for the range $10 - 10^7$Hz using an Impedance Analyzer.

about $\pm 30\%$ is found resulting mainly from the uncertainty of the geometrical parameters involved.

b. Measurements in the range $10^6 - 10^9$ Hz Reflectometers

For frequencies between 10 MHz and 1 GHz reflectometer techniques are used to study the dielectric dispersion of materials including composites [9,25,26,27]. The complex permittivity is obtained by measuring the reflection coefficient at a particular reference plain [26]. The sample is mounted at the end of a coaxial line. Different sample configurations are possible [28]. For solid materials disk shaped samples with metal deposited electrodes can be placed as being part of the coaxial line. A scheme showing a typical sample arrangement is shown in Fig. 7.2. A radio frequency electromagnetic wave is transmitted across the coaxial line. The reflected wave from the sample is lead to a vector voltmeter by using a directional bridge, where it is compared with a reference channel. The reflection coefficient Γ is the ratio between amplitudes of the reflected and incident waves. According to the transmission line theory [28,30]. the reflection coefficient is given by:

$$\Gamma = \frac{Z - Z_0}{Z + Z_0} = |\Gamma| e^{-i\theta} \tag{11}$$

Where Z and Z_0 are sample impedance and short circuit impedance respectively. Taking into account that $Z = \frac{1}{i\omega^* C_0}$, then (11) can be

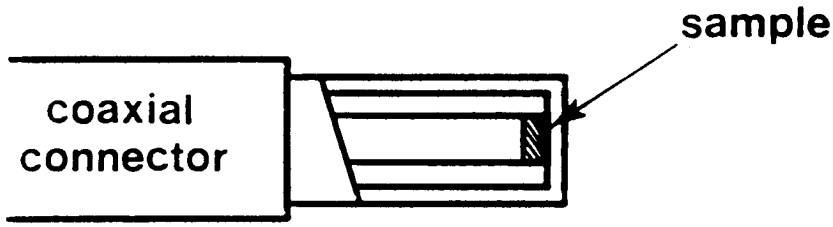

Figure 7.2 Experimental set-up for ac measurements in a reflectometer. Samples are placed as a part of the inner conductor in a coaxial cell.

solved [31]to give:

$$\epsilon' = \frac{2 \mid \Gamma \mid \sin\theta}{\omega C_0 Z_0(\mid \Gamma \mid^2 + 2 \mid \Gamma \mid \cos\theta + 1)} \tag{12}$$

$$\epsilon'' = \frac{1 - \mid \Gamma \mid^2}{\omega C_0 Z_0(\mid \Gamma \mid^2 + 2 \mid \Gamma \mid \cos\theta + 1)} \tag{13}$$

The ac conductivity can be calculated as usual from $\sigma' = \epsilon_0 \epsilon'' \omega$. The accuracy in σ' and ϵ' is about ± 40 % mainly resulting from uncertainties in the determination of the geometrical parameters. The effect of sample dimensions on the measurement accuracy has been extensively described in reference 31. The analyzer must be calibrated with short, open and 50 Ω known standard resistors. An HP 4191A typical experimental set-up is shown in Fig. 7.3.

c. Measurements at 10^{10} Hz *Cavity Perturbation Method*

Measurements of the ac conductivity in the region of 10 GHz are possible by using the cavity perturbation technique [32]. A sample is placed in the center of the rectangular reflection cavity which has a characteristic resonant frequency ω_0'. The presence of the sample shifts the resonant frequency of the cavity by:

$$\delta = \frac{\omega_0' - \omega_0''}{\omega_0'} \tag{14}$$

and the loss factor $1/Q'$ by $\Delta = 1/Q'' - 1/Q'$, where ω_0'' and Q" are the resonant frequency and the Q-value of the cavity with sample. For

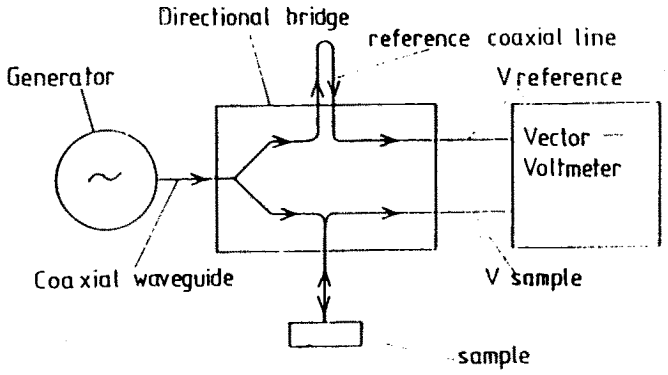

Figure 7.3 Experimental set-up for the frequency range $10^6 - 10^9$Hz.

dielectric solids the electric field at the cavity center totally penetrates the sample. In the static approximation the field inside the specimen can be calculated [33] from:

$$\vec{E} = \frac{\vec{E}_0}{1 + N(\epsilon^* - 1)} \tag{15}$$

where $\vec{E}_0$ is the field in the cavity without sample and N the depolarization factor. For highly conducting samples, like metals, the electric field is rapidly attenuated at the sample surface due to the skin effect [34]. The damping distance, known as skin depth, is given by [35]:

$$\delta' = \left(\frac{2}{\omega\sigma\mu_0}\right)^{1/2} \tag{16}$$

in this case a surface impedance treatment has been developed which allows to obtain the microwave conductivity for highly conducting samples [36,37]. The quasistatic approximation is valid as far as the sample thickness is smaller than the skin depth. For a non magnetic material, $\mu = \mu_0$, at a microwave frequency of 10 GHz a skin depth of 0.1 cm is derived from (16) for a conductivity of 0.1 S/cm. The conductivity range covered by composite materials allows to use the quasistatic approximation by choosing appropriate sample dimensions according to (16). In this case ϵ' and ϵ'' are analytically related with characteristic cavity magnitudes [32] by:

$$\delta = \frac{\alpha}{N}\left(1 - \frac{1 + N(\epsilon' - 1)}{(1 + N(\epsilon' - 1))^2 + (N\epsilon'')^2}\right) \tag{17}$$

$$\delta = \frac{2\alpha}{N} \frac{N\epsilon''}{(1 + N(\epsilon' - 1))^2 + (N\epsilon'')^2)} \tag{18}$$

where α is the filling factor of the cavity and N the depolarization factor. One of the advantages of this method is that no contacts are needed. However the accurate calculation of N is only possible for particular geometries as spheres or ellipsoids. For other shaped samples N has to be calculated by approximation to ellipsoids. Ambiguities in evaluating the conductivity due to less well defined depolarization factors N of non-ellipsoidal samples can be overcome with the help of a fitting procedure [32].

7.3 Experimental Results

a. DC Conductivity in Insulator-Conductor Composite Materials: Carbon-Black Composites

A composite material can be defined as the combination of two or more materials present as separated phases and combined to form structures that may improve certain desirable properties of each individual component [38]. The addition of conducting solid additives such as carbon black, carbon fibers or metallic powders to insulating matrices, mainly polymeric, raises the dc conductivity of the composite towards the conductivity of the additive [38,39,40,41,42]. It is well known that these solid mixtures undergo a discontinuous transition from insulator to conductor for a given concentration of the additive usually referred as ϕ_c. Composite materials based on carbon black are of special industrial and scientific interest [1]. They have been used for different purposes with the main aim of dissipating static charge [43,44]. Although the conductivity of carbon black is not so high as of that of the metals, they present some advantages due to its small particle size ($\approx 80nm$). In addition the possibility of controlling and modifying the aggregate structure of carbon black permits to control the conductivity of the composite [45]. As an example to describe the characteristic morphology of a carbon black composite a Transmission Electron Microscopy (TEM) micrograph of Poly(carbonate)-carbon black composite is shown in Fig. 7.4. The concentration of carbon black (type XE2 from Phillips Petroleum) is $\phi = 6.4\%$. An homogeneous distribution of carbon black particles of diameter about 70 nm dispersed in the polymeric matrix is observed. Nevertheless, a high

degree of connection is observed giving rise to a great number of chain like agglomerates. The state of agglomeration in the composite can be controlled by the mixing technique employed and by the initial level of aggregation, the so called "structure" of the carbon black additive [3]. This parameter can be characterized by the Dibutyl Phthalate (DBP) take-up [46]. The dc conductivity of this type of composites as a function of the volume concentration exhibits a characteristic behaviour which is illustrated in Fig. 7.5 [47]. In this case the system is a low density Poly(ethylene) (from Alcudia, Spain, $\rho = 0.92 g/cm^3$) and a highly structurated carbon black (XE2, Phillips Petroleum). Behind a critical volume of the filler the overall conductivity of the composite does not differ substantially from the corresponding of the insulating matrix. Above ϕ_c, the dc conductivity rises several orders of magnitude and tends towards the conductivity level of the additive. This very general behaviour has been qualitatively observed in a great number of composite systems [48]. The influence of the initial structure of the carbon black on the conductivity of the composite has been discussed [45-49]. Highly structurated carbon black produces high shear during mixing favoring a homogeneous dispersion. Lower critical concentrations and higher levels of conductivity are observed in these cases. The use, for example, of a carbon black (acetylene black) with low level of structure results in a less connected three dimensional network of particles (as shown in Fig. 7.6). This makes the system to remain on the insulating part of the transition for a similar concentration ($\phi = 6.4\%$) at which the first system (Fig. 7.4) is already conducting. The transport mechanism around the critical concentration has been matter of an active discussion in the last years [50-54]. It is governed by tunneling across insulating layers between particles or aggregates. Because of the small size of the potential barriers between particles, there are thermally activated voltage fluctuations which may be high enough to modulate the tunneling probability. This effect introduces a characteristic temperature variation of the temperature independent traditional tunneling conductivity [53].

b. AC Conductivity in Insulator-Conductor Composites: Carbon-Black, Charge Transfer Complexes and Conducting Polymer Composites.

The most recent work on conducting composites has focused the attention not only on the dc conductivity properties but also on the

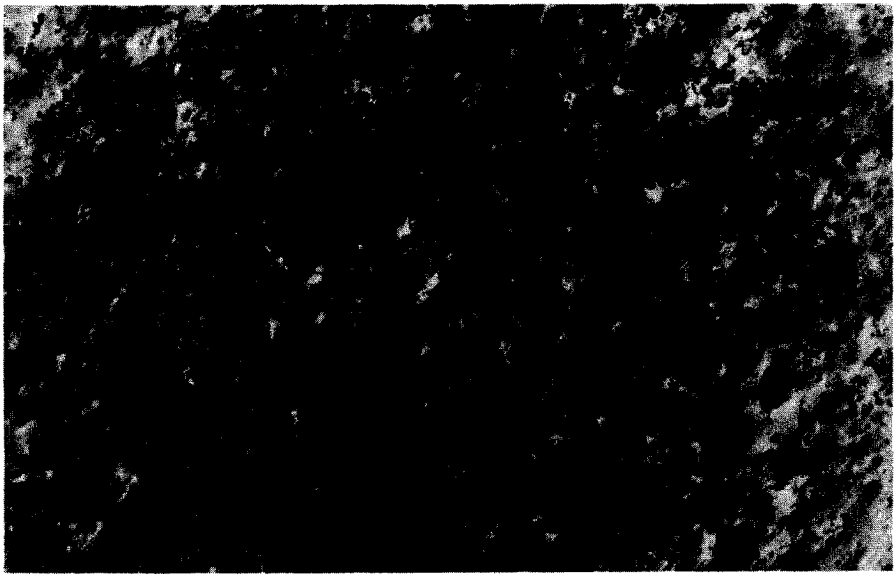

Figure 7.4 TEM micrograph of Poly(carbonate) carbon black (XE2) composite system ($\phi \approx 6.4\%$ vol) (Magnification 7500).

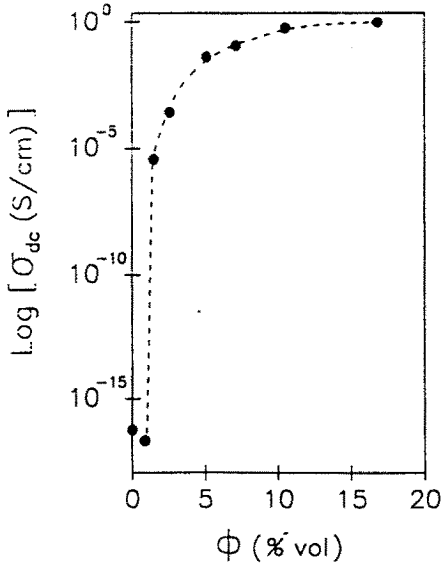

Figure 7.5 Logarithm of the dc conductivity versus volume concentration ϕ for low density poly(ethylene)-Carbon black (XE2) composite.

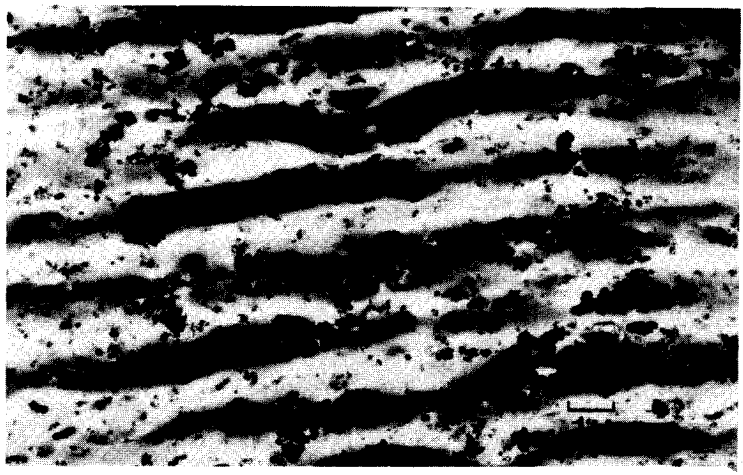

Figure 7.6 TEM of Poly(carbonate)-Carbon black (acetylene black) composite ($\phi \approx 6.4\%$, magnification 7500).

ac conductivity [9,55,56,57]. The use of composites for new applications forces to a better understanding of the processes governing the ac response of these materials. Measurements of both conductivity and permittivity as a function of the frequency have been recently reported [56]. As an example to illustrate the observed frequency dependence, measurements of Low density Poly(ethylene)- carbon black (XE2) composites with $\phi = 1.4\%$ are shown in Fig. 7.7. In this particular case the conductivity exhibits a strong frequency dependence at frequencies higher than 1 kHz starting at 10^{-6} S/cm for 100 Hz and raising up to 10^{-4} S/cm for 10 MHz the relative permittivity decreases with increasing frequency and ranges from about 1000 at 150 Hz to 50 at 10 MHz. The region of strong conductivity frequency dependence depends on the initial dc conductivity of the composite [9, 55-56]. The higher the dc conductivity the less pronounced is the frequency dependence observed. In particular an inversion has been observed at high additive volume concentrations (55). Apart from carbon-black composites other types of advanced composite materials have been recently investigated. Additives which can form charge-transfer complexes (CT) can be grown during a film casting process on a polymeric material like poly(carbonate) or poly(ethylene) [58]. High-conducting polymer films containing precipitates of the charge transfer complexes are obtained under particular preparation conditions [59]. Of especial interest is the control of the morphology of the microcrystalline precipitations when

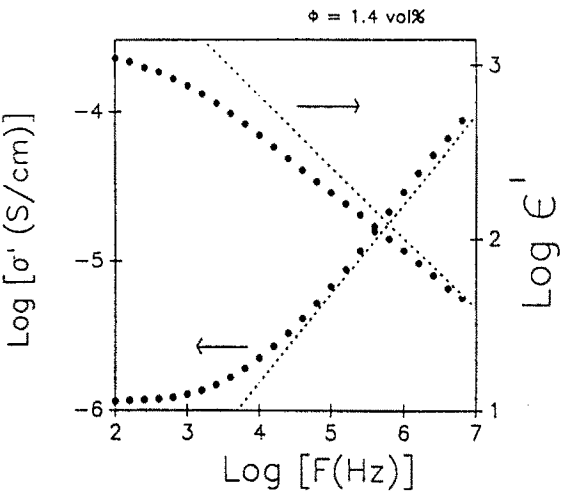

Figure 7.7 Frequency dependence of the conductivity and permittivity at room temperature of PE-Carbon black (XE2) composites ($\phi = 1.4\%$). The dashed lines represent the slopes of 0.6 for σ' and 0.42 for ϵ' expected by the anomalous diffusion model (see text).

the casting procedure is modified [60]. Critical concentrations of about 0.003 volume fraction has been observed depending on the nature of the CT complex and experimental conditions [61]. The frequency dependence of the conductivity of these reticulated doped polymer films has been measured in the range of 1 kHz-10MHz [62]. Some experimental results for different systems are shown in Fig. 7.8. The most striking fact, as compared with the composites based on carbon black, is the absence of frequency dependence in this range of frequencies. The existence of an almost perfect connecting network of conducting microcrystals seems to be responsible for the observed lack of frequency dependence.

Conducting polymers can also be used as additives to build up advanced composites with interesting electrical properties. Poly(acetylene) or Poly(pyrrole) can be incorporated into a thermoplastic matrix by an in situ polymerization process either chemically [63,64] or electrochemically [65]. Conductivities as high as 10 S/cm have been achieved. Moreover, the recent development of conducting polymers which are soluble in the oxidized state [66,67,68] and thus, susceptible to be mixed in solution with thermoplastics has opened the door to a very attractive class of full polymeric conducting composites [69]. In addition some conducting polymers like poly(pyrrole) and poly(aniline)

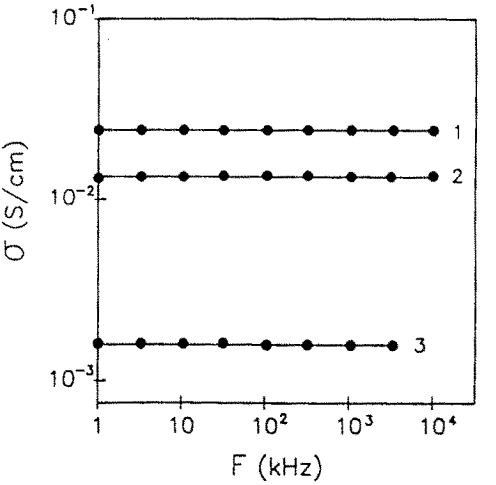

Figure 7.8 Conductivity versus frequency for (1) PE + 1 wt % of TTF-TCNQ and (2) Poly(propylene) + 2 wt % of TTF-TCNQ and (3) Poly (carbonate) + 2 wt % PrPht-$TCNQ_2$, (from ref. 62).

can be obtained in the form of powder and consequently can be used as additive in a similar way as carbon black. The dc conductivity of these systems suffers an insulator-conductor transition qualitatively similar to that of the carbon black composites case [70,71,72]. The frequency dependance of conductivity and permittivity is illustrated in Figs. 7.9–7.14 for three different types of polymeric insulator-conductor composites. In the first case conducting salts of Poly(pyrrole) were prepared by polymerization of pyrrole (PY) (Merck, distilled before used) in aqueous solution by ammonium peroxodisulfate (APS) (from Merck) in the presence of sodium cellulose sulfate (SCS) at the following weight ratios: PY/SCS=0.67, PY/APS=1. Poly(pyrrole) (PPY) is obtained in the form of a black powder with a density of $1.49\,g/cm^{-3}$, $\sigma' = 1\,S/cm$, specific surface (BET) of $34 * 10^4 cm^2/g$ and a mean particle size of about 50 nm as determined by TEM. Composite samples containing up to 40 % in weight of the PPY additive were prepared by mixing the conducting powder with molten Poly(ethyleneoxide) PEO (Polywachs 15590 from Hlls $\rho = 1.22\,g/cm^3$). The samples for electrical measurements up to 1 MHz were molded at $65°C$ in the form of films with a thickness between 0.1 and 0.12 cm. Circular gold electrodes (1 cm diameter) were evaporated on both sides of the sample. The conductivity was measured in the direction perpendicular to the free surface of the sample. Between 1 MHz and 1 GHz disc shaped samples (0.3 cm

of diameter, 0.1 cm thickness) were placed in a coaxial cell as previously described. For the measurements at 10 GHz rectangular strips of $1 * 0.3 * 0.1 cm^3$ were cut from the samples and placed in a rectangular transmission cavity. The cavity was operated in the TE_{103} mode with a resonant frequency of 9.4 GHz [32]. The frequency dependence of the conductivity at room temperature from 10 Hz to 10^{10} Hz is shown in Fig. 7.9 for PEO-PPY composites with increasing volume concentration. The conductivity exhibits a first region in which almost no change with frequency is observed. Subsequently at higher frequencies a stronger frequency dependence appears. As it is shown the lower the additive concentration the broader is the range in which the strong frequency dependence of the conductivity is observed. The permittivity of these composites suffers a decrease with frequency as shown in Fig. 7.10 in the 10 Hz-1MHz frequency range. For a given frequency the higher the volume concentration the higher is the value of the dielectric constant. Very similar features have been observed for a composite system based on Poly(vinylchloride) (PVC) and poly(pyrrole). In this case Poly(pyrrole) was prepared following the same procedure as in the previous case but here without SCS. A black precipitate of PPY is obtained (DBP $\approx 2 cm^3/g$, $\sigma' = 1\,S/cm$). Composites were prepared by suspending PPY in a solution of PVC in Tetrahydrofurane (10%). The solvent was slowly evaporated to obtain thin free standing films of about 0.005 cm. The linear four probe configuration was employed to measure σ' for the highly conducting samples. Thicker films with gold evaporated electrodes were used for samples with lower conductivities. No qualitative difference is observed in the behaviour of conductivity and permittivity at room temperature, Fig. 7.11 and 12, as compared to the previous case. Finally we report measurements carried out on Poly(aniline)-PVC composites submitted to us by Zipperling and Kessler [73]. Conductivity and permittivity as a function of the frequency at room temperature are shown in Figs. 7.13 and 7.14 respectively. The general behaviour does not differ qualitatively from the previous cases.

7.4 Theoretical Approach

a. Effective Medium Theory

The Effective Medium Theory (EMT) has been a classical approximation employed to explain the dielectric dispersion of conductor-

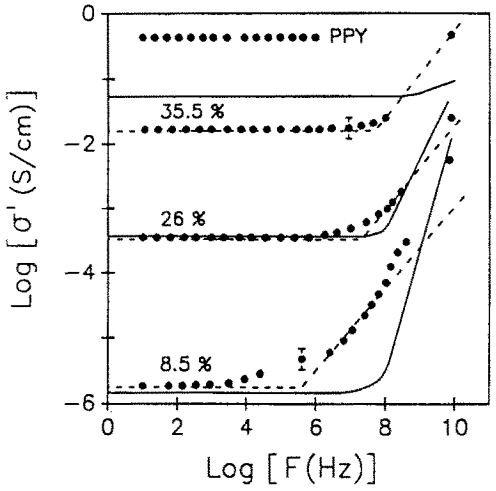

Figure 7.9 Frequency dependence of σ' at room temperature in PEO-PPY composites with different volume concentrations of PPY. The solid lines are fitting curves using Effective Medium Theory according to (19). The following parameters have been used: $\sigma_2(\phi = 8.5) = 10^{-6}; \sigma_2(\phi = 26.8) = 10^{-4}; \sigma_2(\phi = 53.5) = 10^{-2}; \epsilon_{PPY} = 0; \sigma_{PPY} = 1; \epsilon_{PEO} = 10; \mid \sigma \mid =$ S/cm, $\mid \epsilon \mid =$ relative units. The dashed curves represent the expected slope under the predictions of anomalous diffusion in percolation clusters (see text).

insulator composites [74,75,76]. The mathematical method developed by Bruggeman assumes that the two phases of the mixture are of spherical nature. According to this theory the conductivity and dielectric constant of a binary phase composite are governed by the equation:

$$\phi \frac{\epsilon_1^* - \epsilon_m^*}{\epsilon_1^* + 2\epsilon_m^*} = -(1-\phi)\frac{\epsilon_2^* - \epsilon_m^*}{\epsilon_2^* + 2\epsilon_m^*} \tag{19}$$

where ϵ_1^*, ϵ_2^* and ϵ_m^* are the complex dielectric constant of the two component and composite respectively, ϕ is the volume fraction of the conducting material. Taking into account that $\sigma' = \epsilon'' \epsilon_0 \omega$, (19) can be solved to give both the imaginary and the real part of the dielectric function and consequently the ϵ' and σ' values characteristic of the composite. Inherent to this formulation is the fact that a three dimensional system undergoes an insulator-conductor transition at $\phi = 1/3$. At this point a maximum in ϵ_m' is reached. The magnitude of this maximum depends on both components [55]. The higher the difference between the conductivity the higher the maximum in ϵ_m'. Conductivity

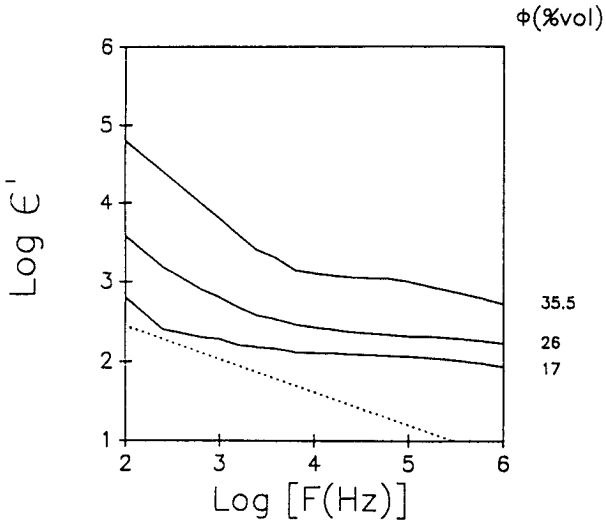

Figure 7.10 Variation of ϵ' with frequency for PEO-PPY composites with different additive concentrations. The dashed line represents the slope expected by the anomalous diffusion model.

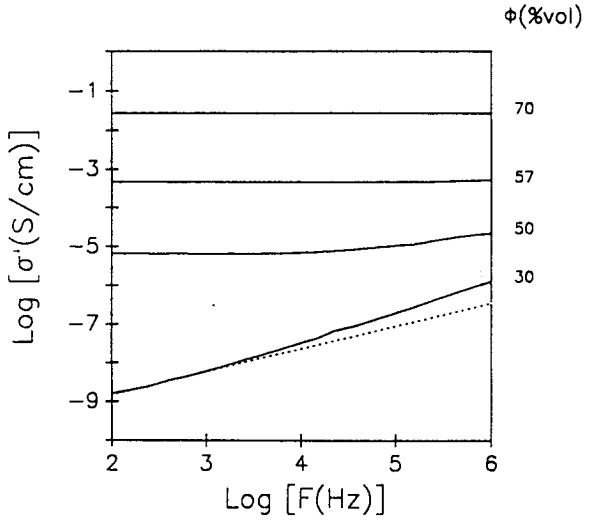

Figure 7.11 Frequency dependence of σ' for PVC-PPY composites at different PPY volume concentrations. The dashed line represents the slope expected by the anomalous diffusion model.

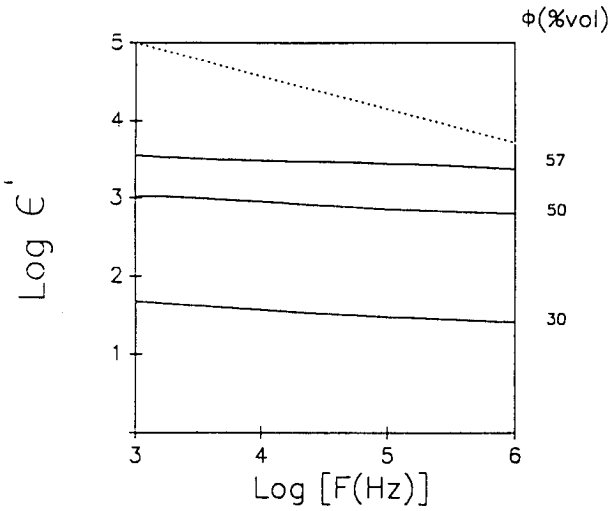

Figure 7.12 Variation of ϵ' with frequency for PVC-PPY composites for different PPY volume concentrations. The dashed line represents the slope expected by the anomalous diffusion model.

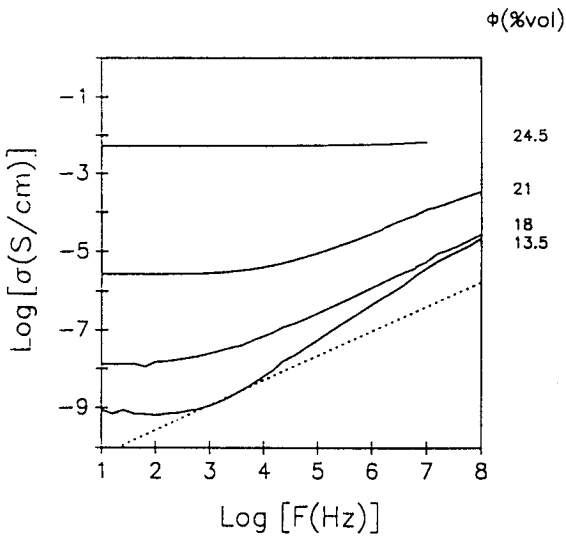

Figure 7.13 Frequency dependence of σ' for PVC-PANI composites for different additive concentrations. The dashed line represents the slope expected by the anomalous diffusion model.

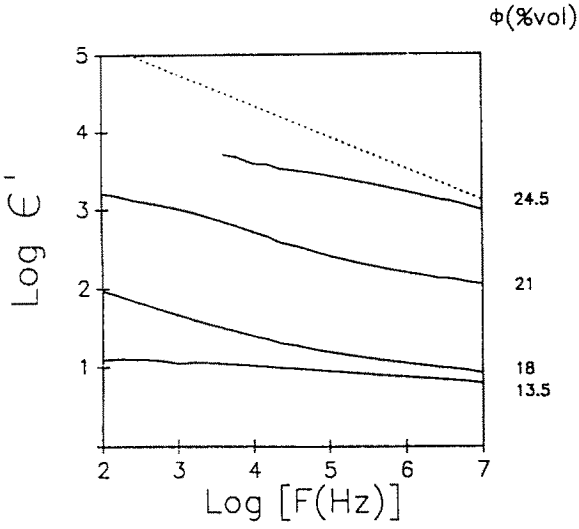

Figure 7.14 Variation of ϵ' with frequency for PVC-PANI composites at different PANI concentrations. The dashed line represents the slope expected by the anomalous diffusion model.

and dielectric constant exhibit a strong frequency dependence when a characteristic frequency is achieved. This behaviour is shown in Fig. 7.15 for a particular choice of the parameters involved on the model. As it is shown the conductivity of the less conductive component controls the conductivity of the system at low frequencies. When the difference in conductivities increases a progressively slower frequency dependence appears. EMT has been successfully used to explain the frequency dependence of the conductivity in spherical carbon black composites (9). However, chain-like structurated carbon black composites, which tend to form well connected networks even at low levels of concentrations, depart from what EMT predicts (55). Equation (19) has been used in an attempt to fit the experimental results of conductivity for the PPY-PEO system under the EMT considerations with different fitting parameters [77]. The result of the fitting procedure is shown in Fig. 7.9 by the continuous lines. The parameters used in this case have been written on the legend. The particular choice of σ_2 conductivities has been made by considering the possibility of interparticle conduction mechanism like tunneling or hopping. This effect makes the system to be considered as a binary mixture. One conducting phase (PPY) and a less conducting phase characterized not by the conductivity of

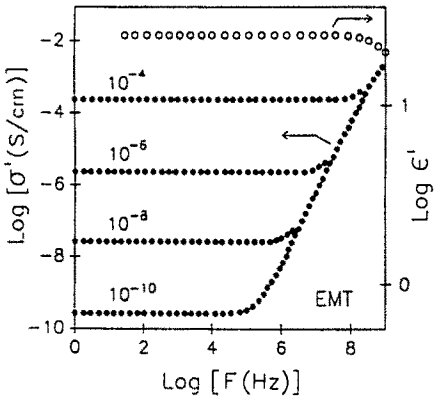

Figure 7.15 Frequency dependence of $\sigma'(\bullet)$ and $\epsilon'(\circ)$ expected by the Effective Medium Theory (EMT). The parameters used in this plot are: $\sigma_1 = 0.1$, $\epsilon_1 = 0$, $\epsilon_2 = 0$, $\phi = 0.2$ and σ_2 varying according with the numbers labeled on the figure.

the matrix but for the conductivity of the gaps between particles. In this case the low frequency experimental conductivity has been taken as σ_2. As it is shown no correlation between experience and theory is found over the broad range of frequency investigated. The deviation from sphericity of the PPY additive [77] might cause the reported disagreement.

b. Percolation Theory

Conductivity and permitivity of insulator-conductor composites can be analyzed by the percolation theory which has been actively studied in the last years (6–8). According to this approach the bulk conductivity of a composite system suffers an insulator-conductor transition at a critical volume concentration ϕ_c of the conducting phase. At this point charge carriers percolate through a continuous infinite network of conducting elements which are in physical contact. After ϕ_c is achieved the conductivity scales as:

$$\sigma' \propto (\phi - \phi_c)^{\mu} \tag{20}$$

and before ϕ_c the permittivity follows the scaling relation :

$$\epsilon' \propto | \phi - \phi_c |^{-s} \tag{21}$$

These scaling laws are valid for ϕ in the proximity of ϕ_c. Current values of μ between 1.5 and 2, and of $s = 0.7$ have been reported

on three dimensional systems [6,8,78]. Although ϕ_c depends on the geometrical details of the system, the critical exponents μ and s are "universals", i.e. dependent only on the dimensionality of the system (6). Nevertheless, experimental and theoretical studies suggest that they can take, in particular cases, higher values than the "universals" [79,80]. In particular, attempts to fit (20) to experimental systems have been made (72). The existence of interparticle conduction effects, like tunneling, makes the system to become conductor before a physical contact between particles has been achieved (53). Another important magnitude that characterizes the composite system in the vicinity of ϕ_c is the correlation or connectivity length ξ. The scaling law followed by ξ is:

$$\xi \propto | \phi - \phi_c |^{-\nu} \tag{22}$$

with $\nu \approx 0.88$ in three dimensions. This magnitude is correlated to many intrinsic properties of the multicomponent system and can be envisioned as proportional to the mean size of the clusters present in the system at a volume concentration ϕ [81] The dependence with frequency of σ' and ϵ' may result from two effects: (a) anomalous diffusion in the clusters [11,82,83] and (b) polarization of the insulating matrix between clusters [84].

The fractal nature of the percolating network for length scales smaller than ξ (82) implies some important features for the conductivity and permittivity. The time employed by a charge carrier to move an Euclidian distance r in the fractal cluster is $t \propto r^{d_w}$ with $d_w > 2$ instead of the classical square dependence. Here d_w is the fractal dimension of the trajectory of a random walker placed on a fractal object (10–11). This effect is referred as anomalous diffusion in opposition to a normal diffusion process in which $t \propto r^2$. This anomalous diffusion give rise to scaling relations for conductivity and permittivity in the following way (82–83) :

$$\sigma' \propto \omega^x \tag{23}$$

for frequencies $\omega > \omega_\xi \propto \xi^{-d_w}$ with $x = \mu/(\nu d_w) \approx 0.6$ and:

$$\epsilon' \propto \omega^{-y} \tag{24}$$

with $y = s/(\nu d_w) \approx 0.4$ in three dimensions.

When inter-cluster polarization effects are considered similar scaling relations for x and y are obtained but higher values for $x = 0.72$

and lower for $y = 0.28$ have been deduced (56, 84). The two critical exponents are supposed to follow the equation :

$$x + y = 1 \tag{25}$$

Experimental work has been made in connection with these theoretical approaches. Two dimensional very thin films obtained by evaporation of gold onto insulating substrates result in systems geometrically close to an ideal percolation system [83,85]. Although the power law behaviour predicted by (23), (24) and (25) was observed, significant differences of the exponent values have been detected as compared with the theory. Similarly in three dimensional carbon black-teflon composites the power law behaviour has been found although a quantitative disagreement theory-experiment in the exponents remains (56).

From the analysis of the experiments performed in the polymer-conducting polymer composites the power law behaviour predicted by (23) and (24) can be qualitatively observed. In order to compare the experimental of σ' and ϵ' with the mean theoretical exponent predicted by the anomalous diffusion considerations dashed lines with slopes 0.6 and 0.4 have been drawn in Figs. 7.7, 7.9–7.14. For the carbon black composite (Fig. 7.7) the conductivity follows the theoretical predictions after that a critical frequency of 10^4 Hz has been achieved. The permittivity exhibits a deviation at low frequencies but the limit slope at higher frequencies is very closed to the y = 0.4 predicted value. In this case the scaling relation 23, 24, and 25 can be considered as experimentally fulfilled in this range of frequencies. By looking at the conductivity of the PPY-PEO composites (Fig. 7.9) some interesting features can be discussed. In samples with low concentrations only a small region (10^6–10^8 Hz) seems to follow the $x = 0.6$ dependence. At higher frequencies a stronger frequency dependence is observed giving rise to higher slopes. When the concentration is increased this region shifts to higher frequencies and the experimental slope follows over a broader range of frequencies the 0.6 value. The frequency dependence for the other two types of composite exhibits qualitatively the same behaviour. As it is shown in Figs. 7.11 and 7.13, the higher the volume concentration of the conducting additive the less pronounced is the frequency dependence. In relation to the permittivity (Figs. 7.10, 7.12 and 7.14) a decrease with increasing frequency as predicted by (24) is observed. However, an experimental slower dependence is observed as compared with the $y = 0.4$ theoretical prediction. Only for

the higher concentrations at low frequencies (Figs. 7.10 and 7.14) the experimental slopes roughly approximate the 0.4 value.

The experimental frequency dependence of the conductivity in this type of three dimensional composites reflects a continuous process. At low frequencies, the charge carriers are supposed to follow a normal diffusion process and no dispersion of the conductivity is expected in good agreement with the experimental results. The charge carriers are forced to move over large distances compared to the mean cluster size and the macroscopic conductivity is controlled by tunneling or hopping between clusters. Due to this fact electrical conduction is possible before the physical contact between particles at ϕ_c has been achieved. When the frequency is increased the mean displacement r of the charge carriers is reduced, in particular when $r \ll \xi$ the conductivity is governed by (23) due to the fractal nature of the clusters. When the concentration increases the percolation network becomes less tortuous and smaller length scales i.e. higher frequencies are needed to detect an anomalous diffusion process. This fact might result on the decrease of the frequency dependence observed when the filler concentration is increased. The effective size of the cluster has to be understood by considering all the cluster which are connected by tunneling or hopping and is higher than the size of the real clusters formed by physically contacted particles. Finally at higher frequencies the polarization of the matrix between clusters acting like a capacitor network can give rise to a no negligible parallel contribution to the ac conductivity due to the displacement current and might be responsible for the higher than 0.6 slopes experimentally observed. The experimental increase of the permittivity with the volume concentration ϕ of the conducting component observed in the three systems can be interpreted by considering a conducting network of clusters stretching across the sample and interrupted by thin dielectric films of the matrix. These clusters contribute to the conductivity because they are electrically connected, but also contribute to ϵ' giving a very large capacitance. This fact provides an additional support to the tunneling or hopping conduction hypothesis before ϕ_c is achieved. A very simple scheme of this model is depicted in Fig. 7.16a. Isolated clusters A together with electrically connected clusters B through the junctions J result in an equivalent circuit as schematically shown in Fig. 7.16b. At higher concentrations when the physical contact between clusters occurs a decrease in ϵ' should be expected. As shown in Figs. 7.10, 7.12 and 7.14, when the

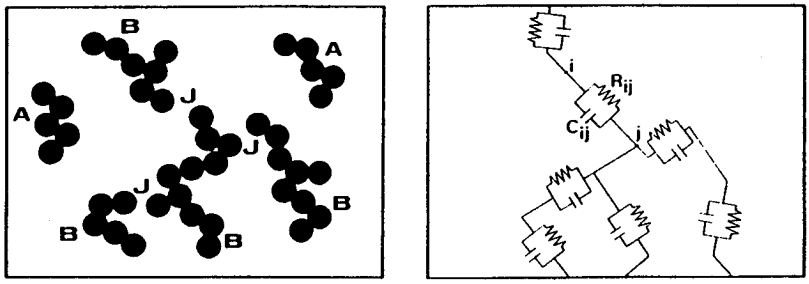

Figure 7.16(a) Schematic model showing two types of clusters: isolated clusters (A) and clusters (B) electrically connected through the (J) junctions. (b) Equivalent circuit corresponding to the model.

filler concentration increases a higher frequency dependence in ϵ' appears especially visible at low frequencies. This opposite tendency as compared with the behaviour of the conductivity may be an indication that the fractal character of the capacitive and conductive network formed by the clusters changes in a different way when the additive concentration is increased.

7.5 Conclusions

The ac electrical conductivity of insulator-conductor composites has been described in the frequency range from $10 - 10^{10}$ Hz. Three measuring techniques have been used to measure conductivity and permittivity as a function of the frequency. The dc electrical properties of insulator-conductor composites have been commented and illustrated for carbon black composites. The ac conductivity and permittivity of traditional carbon black composites and new advanced composites based on charge transfer complexes and conducting polymers have been shown. The ac conductivity exhibits a strong frequency dependence when a critical frequency has been reached. The frequency dependence of the conductivity become less pronounced when the additive concentration is increased. The permittivity decreases with increasing frequency and the dependence becomes stronger at low frequencies when the additive concentration increases. For a given frequency an increment of ϵ' was also observed when the filler concentration was in-

creased. The experimental results have been discussed in the light of the Effective Medium Theory (EMT) and Percolation Theory (PT). Although EMT has been used sometimes to explain the behaviour of σ' and ϵ' in carbon black composites no agreement has been found for the polymer-conducting polymer systems. In this case the ac conductivity is shown to follow the general law $\sigma' \propto \omega^x$ for frequencies higher than a critical. For every concentration of the conducting additive a frequency region has been found where the predictions for anomalous diffusion in fractal percolation clusters, ($x = 0.6$), can be considered as fulfilled. The stronger frequency dependence observed at higher frequencies can be interpreted as being due to polarization effects of the thin polymeric films of the matrix between clusters. The capacitive contribution of the observed increment of ϵ' with increasing volume concentration. The frequency dependence of ϵ' qualitatively follows a general law $\epsilon' \propto \omega^{-y}$. The experimental slopes only at low frequencies roughly approximate the predictions for anomalous diffusion indicating that probably polarization effects are predominant for ϵ' in the investigated range of measurements. The extension of the described experiments to lower frequencies and to other types of composite systems will undoubtedly shed additional light to the still growing field of research on the electromagnetic propagation in conducting composite materials.

Acknowledgements

T.A. Ezquerra is indebted to the Max-Planck-Gesellschaft (F. R.G.) and to C.S.I.C. (Spain) for financial support. Thanks are also given to Prof. F.J. Baltá-Calleja and Dr. M. Sanchez-Cuesta for scientific and technical assistance.

References

[1] *Carbon black Polymer Composites*, E. K. Sichel Ed., Marcel Dekker, New York 1982.

[2] *Conductive Polymers*, R. B. Seymour Ed., Plenum Press, New

York 1981.

[3] Manson, J. A., and L. H. Sperling, *Polymer Blends and Composites*, Plenum Press, New York 1976.

[4] *Carbon Fibers and their Composites*, E. Fitzer Ed., Springer Verlag, Berlin 1985.

[5] Hull. *An Introduction to Composite Materials*, Cambridge University Press, London 1981.

[6] Stauffer, D., *Introduction to Percolation Theory*, Taylor & Francis, London 1985.

[7] Kirkpatrick, S., *Rev. Mod. Phys.* **45**, 547, 1973.

[8] Stauffer, D., *Phys. Rep.*, **54**, 1, 1, 1979.

[9] Kawamoto, H., *Carbon black Polymer Composites*, E.K. Sichel Ed., Marcel Dekker, New York, 35, 1982.

[10] Liu, S. H., *Solid State Physics, Advances in Research and Applications*, H. Ehrenreich, D. Turnbull Ed., Academic Press, New York, 267, 1986.

[11] Stanley, H. E., *On Growth and Form*, H. E. Stanley, N. Ostrowsky Ed., Martinus Nijhoff Publishers, Boston, 21, 1986.

[12] Böttcher, C. J. F., and P. Bordewijk,*Theory of Electric Polarization*, Elsevier, Amsterdam, 12, 1978.

[13] Blythe, A. R., *Electrical Properties of Polymers*, Cambridge University Press, London, 39, 1979.

[14] Cohen, R. W., G. D. Cody, M. D. Coutts, and B. Abeles, *Phys. Rev. B*, **8**, 3689, 1973.

[15] Valerien, S. U., F. Kremer, and C. Boeffel, *Liquid Crystals*, **4**, 1, 79, 1989.

[16] Boese, D., F. Kremer, and L. J. Fetters, *Makromol. Chem., Rapid Commun.*, **9**, 367, 1988.

[17] Valerien, S. U., F. Kremer, H. Kapitzc, R. Zentel, and W. Frank, *Physics Letters A*, **138**, 4, 219, 1989.

[18] Seanor, D. A., *Electrical Properties of Polymers*, Academic Press Inc., Chap. 1, (1982).

[19] Kryszewski, M., *Semiconducting Polymers*, PWN-Polish Scientific

Publishers, Warszawa, 401, 1981.

[20] Field, R. F., *Dielectric Materials and Applications*, R. von Hippel Ed., Chapman&Hall, London, 47, 1954.

[21] Valdes, L. B., *Proc. IRE*, **42(2)**, 420, 1954.

[22] Montgomery, H. C., *Appl. Phys.*, **42**, 7, 2971, 1971.

[23] van der Pauw, L. J., *Phillips Res. Rept.*, **16**, 187, 1961.

[24] Ulanski, J., D. T. Glatzhofer, and G. Wegner, *Makromol. Chem., Rapid Commun.*, **7**, 361, 1986.

[25] Whitathey, T., M. A. Stuchly, and S. S. Stuchly, *IEEE Trans. Microwave Theory Tech.*, **MTT-30**, 1, 82, 1982.

[26] Stuchly, S. S., M. A. Rzepecka, and M. F. Iskander, *IEEE Trans. Instrum. Meas.*, **IM-23**, 1, 56, 1974.

[27] Böhmer, B., M. Maglione, P. Lunkenheimer, and A. Loidl, *J. Appl. Phys.*, **65(3)**, 901, 1989.

[28] Stuchly, M. A., and S. S. Stuchly, *IEEE Trans. Instrum. Meas.*, **IM–29**, 3, 176, 1980.

[29] Barlow, H. M., and A. C. Cullen, *Microwave Measurements*, Constable & Co ltd., London, 1950.

[30] von Hippel, R., *Dielectric Materials and Applications*, Chapman & Hall, London, 13, 1954.

[31] Rzepecka, M. A., and S. S. Stuchly, *IEEE Trans. Instrum. Meas.*, **IM-24**, 1, 27, 1975.

[32] Bauhofer, W., *J. Phys. E: Sci. Instrum.*, **14**, 934, 1981.

[33] Kittel, C., *Introduction to Solid State Physics*, John Wiley&Sons Inc., 1956.

[34] *Principles of the Theory of Solids*, J. M. Ziman, Cambridge University Press, 241, 1965.

[35] Solymar, L., and D. Walsh, *Lectures on the Electrical Properties of Materials*, Oxford University Press, 12, 1984.

[36] Cohen, M., S. K. Khanna, W. J. Gunning, A. F. Garito, and A. J. Heeger, *Solid State Commun.*, **17**, 367, 1975.

[37] Khanna, S. K., E. Ehrenfreund, A. F. Garito, and A. J. Heeger, *Phys. Rev. B*, **10**, 2205, 1974.

[38] *Encyclopedia of Composite Materials and Components*, J. Wiley &Sons, New York, 1986.

[39] Garland, J., *Trans. of Met. Soc. of AIME*, **235**, 642, 1966.

[40] Bueche, F., *J. Appl. Phys.*, **44**, 532, 1973.

[41] Aharoni, S. W., *J. Appl. Phys.*, **43**, 5 1972.

[42] Kusy, R. P., *J. Appl. Phys.*, **48**, 12, 5301, 1977.

[43] Swor, R. A., D. R. Harris, and F. Lyon, *Kautschuk+Gummi. Kunstoffe*, **37**, 198, 1984.

[44] Moebius, K. H., *Kunststoffe*, **78**, 1, 53, 1988.

[45] Jantzen, J., *J. Appl. Phys.*, **46**, 2, 966, 1975.

[46] Medalia, A. I., 1 in ref 1.

[47] Ezquerra, T. A., F. J. Baltá-Calleja, and J. Plans, *J. Mater. Res.*, **1**, 510, 1986.

[48] Clarke, P. S., J. W. Orton, and A. J. Guest, *Phys. Rev. B*, **18**, 1813, 1978.

[49] Ezquerra, T. A., J. Martinez-Salazar, and F. J. Baltá-Calleja, *J. Mater. Sci. Lett.*, **5**, 1065, 1986.

[50] Quivy, A., R. Deltour, A. G. M. Jansen, and P. Wyder, *Phys. Rev. B*, **39**, 1026, 1989.

[51] Sheng, P., E. K. Sichel, and J. I. Gittleman, *Phys. Rev. Lett.*, **40**, 1197, 1978.

[52] Sichel, E. K., J. I. Gittleman, and P. Sheng, *Phys. Rev. B*, **18**, 5712, 1978.

[53] Sheng, P., *Phys. Rev. B*, **21**, 2180, 1980.

[54] Sichel, E. K., J. I. Gittleman, and P. Sheng, *J. of Electro. Mat.*, **11**, 699, 1982.

[55] Chung, K. T., A. Sabo, and A. P. Pica, *J. Appl. Phys.*, **53**, 10, 1982.

[56] Song, Y., T. W. Noh, S. Lee, and J. R. Gaines, *Phys. Rev. B*, **33**, 904, 1986.

[57] Chung, K. T., *Org. Coat. Appl. Polym, Sci. Proc.*, **48**, 660, 1983.

[58] Jeszka, J. K., J. Ulanski, and M. Kryszewski, *Nature*, **289**, 390,

1981.

[59] Kryszewski, M., J. K. Jeszka, J. Ulanski, and A. Tracz, *Pure& Appl. Chem.*, **56**, 355, 1984.

[60] Burda, L., A. Tracz, T. Pakula, J. Ulanski, and M. Kryszewski, *J. Phys. D: Appl. Phys.*, **16**, 1737, 1983.

[61] Ulanski, J., A. Tracz, and M. Kryszewski, *J. Phys. D: Appl. Phys.*, **18**, 451, 1985.

[62] Ulanski, J., M. Kryszewski, A. Tracz, and F. Kremer, *Synth. Met.*, **24**, 89, 1988.

[63] Wnek, G. E., *Handbook of Conducting Polymers*, T.A. Skotheim Ed., Marcel Dekker, New York, 205, 1986.

[64] Pron, A., and K. Wojnar, *Electronic Properties of Conjugated Polymers*, H. Kuzmany, M. Mehring, S. Roth Ed., Springer Verlag, Berlin, 291, 1987.

[65] Lindsey, S. E., and G. B. Street, *Synth. Met.*, **10**, 67, 1984.

[66] Rughooputh, S. D. D. V., M. Nowak, S. Hotta, A.J. Heeger, and F. Wudl, *Synth. Met.*, **21**, 41, 1987.

[67] Rühe, J., T. A. Ezquerra, and G. Wegner, *Makromol. Chem., Rapid Commun.*, **10**, 103, 1989.

[68] Rühe, J., T. A. Ezquerra, and G. Wegner, *Synth. Met.*, **28**, C177, 1989.

[69] Österholm, J. E., J. Laakso, P. Nylhom, H. Isotalo, H. Stubb, and O. Inganäs, W. R. Salanek, *Synth. Met.*, **28**, C435, 1989.

[70] Ezquerra, T. A., M. Mohammadi, F. Kremer, T. A. Vilgis, and G. Wegner, *J. Phys. C: Solid State Phys.*, **21**, 745, 1988.

[71] Wessling, B., *Kunststoffe*, **10**, 930, 1986.

[72] Ezquerra, T. A., F. Kremer, M. Mohammadi, J. Rühe, G. Wegner, and B. Wessling, *Synth. Met.*, **28**, C83, 1989.

[73] Wessling, B., H. Volk, *Synth. Met.*, **18**, 671, 1987.

[74] Bruggeman, D. A. G., *Ann. Phys. (Leipzig)*, **24**, 636, 1935.

[75] Landauer. R., *J. Appl. Phys.*, **23**, 779, 1952.

[76] Springett, B. E., *Phys. Rev. Lett.*, **31**, 24, 1463, 1973.

[77] Kremer, F., T. A. Ezquerra, M. Mohammadi, W. Bauhofer, T. A. Vilgis, and G. Wegner, *Solid State Comm.*, **66**, 153, 1988.

[78] Böttger, H., and V. V. Bryksin, *Hopping Conduction on Solids.* VCH Verlaggesellschaft, Weinheim, D.R.G., 120, 1986.

[79] Kohnt, P. M., and J. P. Straley, *J. Phys. C: Solid State Phys.*, **12**, 2152, 1979.

[80] Lee, S., Y. Song, T. W. Noh, X. Chen, and J. R. Gaines, *Phys. Rev. B*, **34**, 6719, 1986.

[81] see 62 in ref 6.

[82] Gefen, Y., A, Aharony, and S. Alexander, *Phys. Rev. Lett.*, **50**, 77, 1983.

[83] Laibowitz, R. B., and Y. Gefen, *Phys. Rev. Lett.*, **53**, 380, 1984.

[84] Bergman, D. J., and Y. Imry, *Phys. Rev. Lett.*, **39**, 1222, 1977.

[85] Hundley, M. F., and A. Zettl, *Phys. Rev. B*, **38**, 10290, 1988.